and derivatized compounds) are identical for the extant and fossil samples (table S2). The extract of a seed cone of extant *Glyptostrobus pensilis* (Chinese water pine) contained 6,7-dehydroferruginol, ferruginol, sugiol, pimaric acid (b), and 18- or 19-hydroxyferruginol (c), as observed in the Miocene *Glyptostrobus oregonensis* cone, but isochamaecydin and chamaecydin could not be detected (*13*) (fig. S1).

Terpenoids are abundant constituents of extant conifers and are used as chemosystematic characteristics (*18–21*). Ferruginol, 6,7-dehydroferruginol, and sugiol are common in extant conifers, especially in the families Cupressaceae, Taxodiaceae, and Podocarpaceae (*18, 20–22*). The unusual triterpenoids isochamaecydin and chamaecydin have hitherto been identified in only two conifer species, Hinoki cypress (*Chamaecyparis obtusa*) and Sugi cedar (*Cryptomeria japonica*) (*17, 23, 24*). We were able to confirm these findings and identified isochamaecydin and chamaecydin in the extracts of seed cones of both species. *Taxodium, Glyptostrobus*, and *Cryptomeria* were formerly treated as members of the Taxodiaceae, and *Chamaecyparis* was assigned to the Cupressaceae, but Taxodiaceae and Cupressaceae were recently merged into one family, Cupressaceae sensu lato (s. l.) on the basis of morphological and molecular genetic data (*25, 26*). The terpenoid compositions detected here in fossil and extant species of former Taxodiaceae support this merger. The similarity of the terpenoids in *Taxodium* and *Glyptostrobus* is not surprising, as these genera are closely related (*25*). The terpenoid characteristics of fossil *Taxodium balticum* and *Glyptostrobus oregonensis* identified here are thus in accordance with their systematic assignment to the Cupressaceae s. l. based on their morphological characteristics.

The results show that polar natural product precursors can be preserved unaltered in fossil conifers and can be used as chemosystematic markers. The applied methods offer a new approach for studying the (paleo)chemosystematics and phylogeny of conifers. The low degree of degradation observed in the analyzed material may be due to the preservation of terpenoids in resinous plant material where the compounds are probably trapped in the resin and protected from degradation or bonding into kerogen. Furthermore, the clayey sediments should prevent the oxidation of the fossil plant material by oxygen-rich waters.

References and Notes

1. B. P. Tissot, D. H. Welte, *Petroleum Formation and Occurrence* (Springer-Verlag, Berlin, 1984).
2. K. E. Peters, J. M. Moldowan, *The Biomarker Guide: Interpreting Molecular Fossils in Petroleum and Ancient Sediments* (Prentice-Hall, Englewood Cliffs, NJ, 1993).
3. T.-G. Wang, B. R. T. Simoneit, *Fuel* **69**, 12 (1990).
4. B. R. T. Simoneit, *Environ. Sci. Pollut. Res.* **6**, 159 (1999).
5. _____, in *Biological Markers in the Sedimentary Record*, R. B. Johns, Ed. (Elsevier Science, Amsterdam, 1986), pp. 43–99.
6. _____, in *The Handbook of Environmental Chemistry*, vol. 3, part I, A. H. Neilson, Ed. (Springer- Verlag, Berlin, 1998), pp. 175–221.
7. M. Streibl, V. Herout, in *Organic Geochemistry: Methods and Results*, G. Eglinton, M. T. J. Murphy, Eds. (Springer-Verlag, New York, 1969), pp. 401–424.
8. E. W. Tegelaar, J. W. de Leeuw, S. Derenne, C. Largeau, *Geochim. Cosmochim. Acta* **53**, 3103 (1989).
9. D. H. Mai, H. Walther, *Abh. Staatl. Mus. Mineral. Geol. Dresden* **38**, 1 (1985).
10. A. Otto, B. R. T. Simoneit, *Geochim. Cosmochim. Acta* **65**, 3505 (2001).
11. Materials and methods are available as supporting material on *Science* Online.
12. C. J. Smiley, W. C. Rember, in *Late Cenozoic History of the Pacific Northwest*, C. J. Smiley, Ed. (Pacific Division, AAAS, San Francisco, 1985), pp. 95–112.
13. A. Otto, B. R. T. Simoneit, W. C. Rember, in preparation.
14. Z. H. Baset, R. J. Pancirov, T. R. Ashe, in *Advances in Organic Geochemistry 1979*, A. G. Douglas, J. R. Maxwell, Eds. (Pergamon Press, Oxford, 1980), pp. 619–630.
15. A. Otto, H. Walther, W. Püttmann, *Org. Geochem.* **26**, 105 (1997).
16. S. M. Kupchan, A. Karim, C. Marcks, *J. Org. Chem.* **34**, 3912 (1969).
17. W. C. Su, J. M. Fang, Y. S. Cheng, *Phytochemistry* **34**, 779 (1993).
18. H. Erdtman, T. Norin, *Prog. Chem. Org. Nat. Prod.* **24**, 207 (1966).
19. H. Erdtman, *Recent Adv. Phytochem.* **1**, 1 (1968).
20. R. Hegnauer, *Chemotaxonomie der Pflanzen*, vol. 1 (Birkhäuser, Basel, 1962).
21. _____, *Chemotaxonomie der Pflanzen*, vol. 7 (Birkhäuser, Basel, 1986).
22. A. Otto, V. Wilde, *Bot. Rev.* **67**, 141 (2001).
23. Y. Hirose, S. Hasegawa, N. Ozaki, Y. Iitaka, *Tetrahedron Lett.* **24**, 1535 (1983).
24. T. Shibuya, *Phytochemistry* **31**, 4289 (1992).
25. P. A. Gadek, D. L. Alpers, M. M. Haslewood, C. J. Quinn, *Am. J. Bot.* **87**, 1044 (2000).
26. S. J. Brunsfeld *et al.*, *Syst. Bot.* **19**, 253 (1994).

27. We thank H. Walther, W. R. Rember, J. Dehmer, and W. Buechler for supplying fossil and extant plant material. The financial support of A. O. by the Max Kade Foundation, New York, is greatly appreciated.

Supporting Online Material

www.sciencemag.org/cgi/content/full/297/5586/1543/DC1
Materials and Methods
Fig. S1
Tables S1 and S2

22 May 2002; accepted 29 July 2002

Global Biodiversity, Biochemical Kinetics, and the Energetic-Equivalence Rule

Andrew P. Allen,* James H. Brown, James F. Gillooly

The latitudinal gradient of increasing biodiversity from poles to equator is one of the most prominent but least understood features of life on Earth. Here we show that species diversity can be predicted from the biochemical kinetics of metabolism. We first demonstrate that the average energy flux of populations is temperature invariant. We then derive a model that quantitatively predicts how species diversity increases with environmental temperature. Predictions are supported by data for terrestrial, freshwater, and marine taxa along latitudinal and elevational gradients. These results establish a thermodynamic basis for the regulation of species diversity and the organization of ecological communities.

Global gradients in biodiversity exist for all major groups of terrestrial (*1*), freshwater (*2*), and marine taxa (*3*), but the general principles underlying their origin and maintenance remain unclear (*4*, *5*). Here we present a theoretical framework that explains gradients of species diversity in terms of energetics. Our model is derived by extending the well-established "energetic-equivalence rule" (*6*) to include temperature. In its original form, the energetic-equivalence rule states that the total energy flux of a population per unit area, B_T, is invariant with respect to body size. Species of different size have similar values of B_T because individual metabolic rates, B_i, increase with body size, M_i, as $B_i \propto M_i^{3/4}$, whereas population densities per unit area, N_i, decrease with body size as $N_i \propto M_i^{-3/4}$ ($B_T = N_i B_i \propto M_i^{-3/4} M_i^{3/4} = M^0$). This inverse relation between abundance and body size is observed for plants and for endothermic and ectothermic animals; it reflects mechanistic connections between individual metabolic rates, rates of energy flux by populations, and the partitioning of available energy among species in a community (*6*, *7*).

We can extend the energetic-equivalence rule to include temperature by incorporating the biochemical kinetics of metabolism. Recent work has shown that whole-organism metabolic rate varies with body size and temperature as $B = b_o M^{3/4} e^{-E/kT}$ (*8*), where b_o is a normalization constant independent of size

Department of Biology, University of New Mexico, Albuquerque, NM 87131, USA.

*To whom correspondence should be addressed. E-mail: drewa@unm.edu

and temperature ($\sim 2.65 \times 10^{10}$ W $g^{-3/4}$) (*9*). The Boltzmann factor, $e^{-E/kT}$, describes the temperature dependence of metabolic rate, where E is the activation energy of metabolism ($\sim$0.78 eV or $\sim 1.25 \times 10^{-19}$ J) (*9*), k is Boltzmann's constant (8.62×10^{-5} eV K^{-1}), and T is absolute temperature (K). The total energy flux of a population is therefore $B_T = N_i B_i = N_i b_o M_i^{3/4} e^{-E/kT}$, which yields

$$\ln(N_i M_i^{3/4}) = (E/1000k)(1000/T) + C_0 \quad (1)$$

where constancy of $C_0 = \ln(B_T/b_o)$ with respect to temperature follows from our extension of the energetic-equivalence rule. Temperatures of ectotherms are approximately equal to ambient environmental temperatures, T_{env}, whereas temperatures of endotherms are $\sim$40°C. Equation 1 therefore leads to three predictions for the relation between population density and temperature: (i) for ectotherms, the natural logarithm of mass-corrected population density should be a linear function of $1000/T_{env}$; (ii) the slope of this linear relation should be $E/1000k \approx 9.0$ K for both plants and animals because the two groups share similar activation energies for metabolism (*8*); and (iii) for endotherms, mass-corrected population density should be independent of T_{env}.

Abundance data compiled on a variety of plant and animal species provide strong support for all three predictions. First, the natural logarithm of mass-corrected population density for tree species throughout the world shows a positive, linear relation to inverse absolute temperature (Fig. 1A). Second, the 95% confidence interval (CI) for the slope of this relation includes the predicted value of 9.0 K ($\bar{x}$; 95% CI, 7.66 to 10.17). Data on mass-corrected population density for terrestrial vertebrate- and invertebrate-ectotherms also support the first and second predictions (slope $\bar{x}$; 95% CI, 6.61 to 16.88) (Fig. 1B). Finally, in accordance with the third prediction, mass-corrected population density shows no significant relation to environmental temperature for endothermic mammals (slope $\bar{x}$; 95% CI, -0.82 to 2.73) (Fig. 1C).

To control for body temperature, we multiply the population densities in Fig. 1, B and C, by the Boltzmann factor, $e^{-E/kT}$, assuming a temperature of 40°C for mammals and temperatures equal to T_{env} for ectotherms. When temperature-corrected population density is plotted against body size on a natural logarithmic scale, endotherms and ectotherms fall on approximately the same line (Fig. 2). Moreover, the slope of this relation is close to the predicted value of $-3/4$ ($\bar{x} = -0.78$; 95% CI, -0.82 to -0.74). Given that the intercept in Fig. 2 provides an estimate of $C_0 = \ln(B_T/b_o)$, that $e^{C_0} = e^{-19.63} = B_T/b_o = 2.95 \times 10^{-9}$ km^{-2} $g^{3/4}$, and that $b_o \approx 2.65 \times 10^{10}$ W $g^{-3/4}$ (*9*), we can estimate B_T to be $\sim$80 W km^{-2} regardless of taxon, body size, temperature, or geographic location.

Having established temperature invariance for B_T, we can now use the energetic-equivalence rule to predict changes in the diversity of ectotherms along temperature gradients. The average population density in a community composed of J individuals and S species is $\overline{N} = J/AS$, where A is the area of the plot delimiting the community and $J = \sum_{i=1}^{S} N_i A$ (*10*). The average metabolic rate of an ectotherm is $\overline{B} = \overline{B_o} e^{-E/kT_{env}}$, where $\overline{B_o} = b_o \overline{M^{3/4}}$ and is calculated on the basis of the frequency distribution of body sizes for species constituting the community of interest. Holding A constant across community samples, $\overline{B_T} = \overline{N}\,\overline{B} = (J/AS)\overline{B_o} e^{-E/kT_{env}}$ and

$$\ln(S) = (-E/1000k)(1000/T_{env}) + C_1 \quad (2)$$

where $C_1 = \ln[(\overline{B_o}/\overline{B_T})(J/A)]$ is assumed to be independent of temperature. This, in turn, requires two assumptions: temperature invariance for abundance, J/A, and temperature invariance for the average derived from the body size distribution, $\overline{M^{3/4}}$, which affects $\overline{B_o}$. These assumptions are supported by the approximate invariance of plant size and abundance across latitudes (*11*). Still, the model is relatively robust to departures from these two assumptions because richness is predicted to vary exponentially with temperature but less than linearly with both average body size, due to its ¾-power scaling exponent, and total abundance, due to sampling properties of species-abundance distributions (*12*). Thus, for example, the predicted 50-fold increase in tree diversity moving from boreal (-5°C) to tropical (30°C) forests as a consequence of biochemical kinetics ($e^{-E/k(273+30)}/e^{-E/k(273-5)} = 50$) should overwhelm any effects attributable to changes in average tree size or total tree abundance (<threefold) (*11*). We take these two assumptions as working hypotheses for the groups of ectotherms considered here but note that they are not expected to hold true for groups that are narrowly defined (e.g., pine trees) or that are strongly regulated in abundance and/or body size by temperature (e.g., reptiles). The model can be extended to explicitly account for temperature effects on other variables.

Equation 2 yields three predictions for the relation of species diversity to temperature: (i) the natural logarithm of species richness should be a linear function of $1000/T_{env}$ for ectotherms; (ii) the slope should be $-E/1000k \approx -9.0$ K along both latitudinal and elevational gradients in temperature for terrestrial taxa; and (iii) the slope should also be -9.0 K for aquatic taxa because they share a similar activation energy for metabolism (*8*).

We find strong support for predictions (i) and (ii) by using two independent data sets on tree diversity along gradients of latitude in North America and elevation in Costa Rica (Fig. 3, A and B). For both data sets, the relation between the natural logarithm of species richness and inverse absolute temperature is approximately linear, and the slopes are both close to the predicted value of -9.0 K (Table 1).

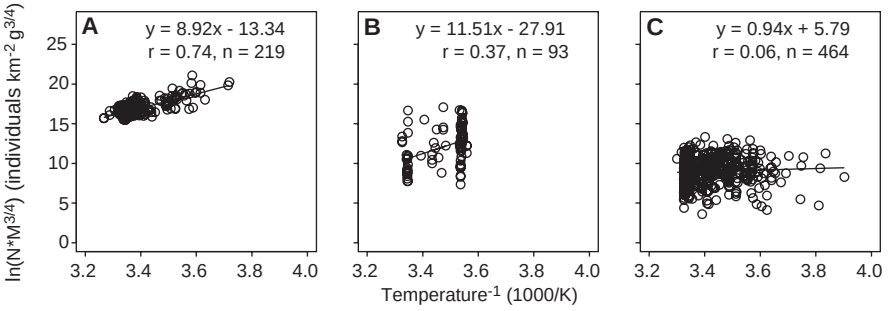

Fig. 1. Effects of average ambient temperature on the natural logarithm of mass-corrected population density for trees (*19*, *22*) (**A**); terrestrial ectotherms including amphibians, reptiles, and invertebrates (*6*) (**B**); and terrestrial mammals from around the world (*6*) (**C**). Temperature estimates were derived from long-term data collected over a global network of stations (*23*). Lines were fitted by ordinary least-squares regression (*24*).

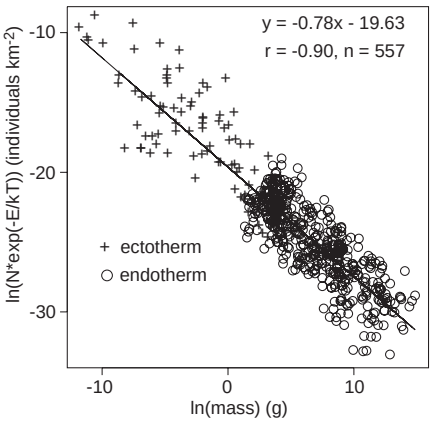

Fig. 2. Effects of body size on temperature-corrected population density for endotherms and ectotherms. The data plotted here are the same as in Fig. 1, B and C. The line was fitted by ordinary least-squares regression (*24*) after applying a natural logarithmic transformation to both variables.

Data on amphibian richness along latitudinal and elevational gradients also support these two predictions with slopes statistically indistinguishable from each other and from those observed for the trees (Fig. 3, C and D). Finally, latitudinal data on riverine fish, marine gastropods, and even the number of fish ectoparasite species per host support all three predictions of the model (Fig. 4). Overall, we see that the slopes are consistently close to the predicted value of –9.0 K ($\bar{x} = -9.21$; range, -7.17 to -10.81), although the confidence intervals do not always include this value.

We do not mean to imply that temperature is the only variable that affects biodiversity. The significant residual variation about the relations in Figs. 3 and 4 emphasizes the importance of other variables including biogeographic history (*13*), habitat heterogeneity (*14*), area (*15*), and geometric constraints on species distributions (*16*). Indeed, we only predict the slopes of the diversity-temperature plots. The intercepts may vary by taxon, habitat, and sampling method. In particular, $\bar{N}$, and therefore $\overline{B_T}$, will vary as functions of plot size A, even if J/A is held constant, because S increases nonlinearly with J as a consequence of sampling, turnover in species composition through space (*12*), and the fractal-like distribution of habitat (*10*, *14*).

Nevertheless, our model accounts for much of the variation in biodiversity (Table 1). Of more importance, it yields testable, quantitative predictions based on first principles of biochemical kinetics and provides a theoretical framework for understanding how temperature and productivity regulate biodiversity. The species-energy hypothesis proposes that biodiversity is positively correlated with productivity because more productive environments contain more individuals and can therefore support more species populations above some minimum size required for persistence (*1*, *17*). Data for endotherms support this hypothesis. The average population densities of mammals are temperature invariant. This implies that the observed increase in mammal diversity toward the tropics (*1*) results from an increase in total density, J/A, for mammals. By contrast, average population densities of trees and other ectotherms show an inverse Boltzmann relation to temperature ($\overline{N} \propto e^{E/kT}$). This result, combined with the observed Boltzmann relation of diversity to temperature for independent data collected on a variety of ectothermic taxa ($S \propto e^{-E/kT}$), supports our model assumption that total ectotherm abundance is approximately independent of temperature ($J/A = \overline{N}S \propto e^{0/kT}$).

Temperature influences the diversity of terrestrial and aquatic ectotherms primarily through its effects on the biochemical kinetics of metabolism. Metabolic rates, in turn, dictate resource requirements at the level of the individual and rates of resource supply required of the ecosystem to maintain communities composed of multiple individuals. Evolutionary rates are ultimately constrained by generation times of individuals and mutation rates. Both of these rates are correlated with metabolic rates and show the same Boltzmann relation to temperature (*9*, *18*). Our results therefore support the hypothesis that elevated temperatures increase the standing stock of species by accelerating the biochemical reactions that control speciation rates (*5*).

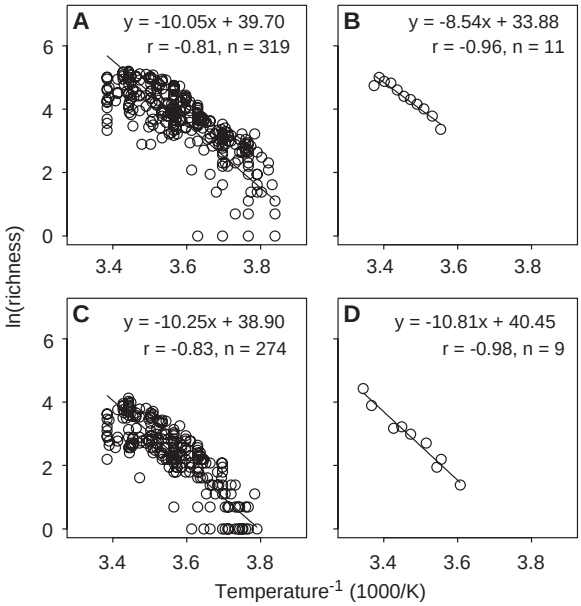

Fig. 3. Effects of mean annual ambient temperature on species richness for North American trees in blocks of 2.5° by 2.5° south of 50°N, and 2.5° (longitude) by 5° north of 50°N (*1*) (**A**); Costa Rican trees along a 2600-m elevational gradient on Volcan Barva (*25*) (**B**); North American amphibians in blocks of 2.5° by 2.5° south of 50°N, and 2.5° (longitude) by 5° north of 50°N (*1*) (**C**); and Ecuadorian amphibians along a 4000-m elevational gradient in the Andes (*26*) (**D**). Temperature estimates were obtained from the sources cited. Lines were fitted by reduced-major-axis regression (*21*, *24*).

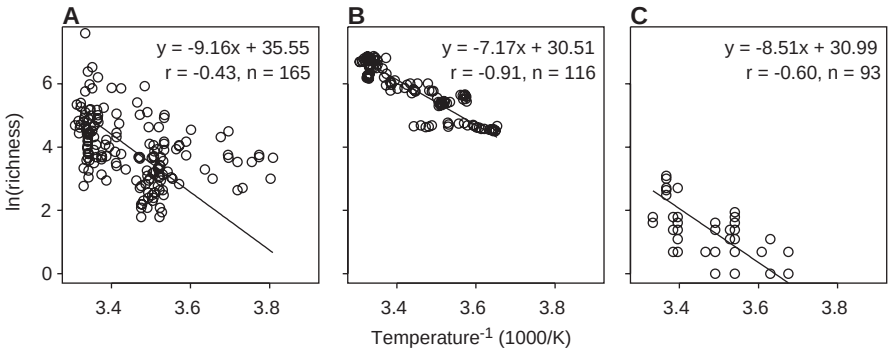

Fig. 4. Effects of mean annual water temperature on richness for fish species in watersheds throughout the world (*2*) (**A**), numbers of marine prosobranch gastropod species per latitudinal degree band along the continental shelves of the Americas (*3*) (**B**), and ectoparasite species per host for marine teleost fish ranging from Antarctica to the tropics (*27*) (**C**). Temperature estimates were obtained from the sources cited. Lines were fitted by reduced–major-axis regression (*21*, *24*).

Table 1. Summary of temperature-biodiversity relations in Figs. 3 and 4, including 95% confidence intervals (CI) for the slope estimates.

Group	Data set	Slope	95% CI	Intercept	*r*	*n*
Trees						
	Latitudinal gradient, North America	−10.05	−10.88 to −9.18	39.70	−0.81	319
	Elevational gradient, Costa Rica	−8.54	−10.10 to −6.48	33.88	−0.96	11
Amphibians						
	Latitudinal gradient, North America	−10.25	−11.01 to −9.58	38.90	−0.83	274
	Elevational gradient, Ecuador	−10.81	−12.10 to −8.83	40.45	−0.98	9
Aquatic taxa						
	Riverine fish, global	−9.16	−11.09 to −7.66	35.55	−0.43	165
	Marine gastropods, Americas	−7.17	−7.65 to −6.71	30.51	−0.91	116
	Marine ectoparasites, Pacific	−8.51	−9.88 to −7.17	30.99	−0.60	93
Average		−9.21			−0.79	

References and Notes

1. D. J. Currie, *Am. Nat.* **137**, 27 (1991).
2. T. Oberdorff, J. F. Guegan, B. Hugueny, *Ecography* **18**, 345 (1995).
3. K. Roy, D. Jablonski, J. W. Valentine, G. Rosenberg, *Proc. Natl. Acad. Sci. U.S.A.* **95**, 3699 (1998).
4. K. J. Gaston, *Nature* **405**, 220 (2000).

5. K. Rohde, *Oikos* **65**, 514 (1992).
6. J. Damuth, *Biol. J. Linn. Soc.* **31**, 193 (1987).
7. B. J. Enquist, J. H. Brown, G. B. West, *Nature* **395**, 163 (1998).
8. J. F. Gillooly, J. H. Brown, G. B. West, V. M. Savage, E. L. Charnov, *Science* **293**, 2248 (2001).
9. Results are based on reduced-major-axis regression analyses of metabolic rate data (*8*) and molecular evolution data in J. F. Gillooly, A. P. Allen, G. B. West, J. H. Brown, in preparation.
10. Estimates of average population density $\bar{N}$, and therefore $\overline{B_T}$, obtained from Damuth's compilation of the published literature (*6*) are not directly comparable to estimates calculated on the basis of number of individuals, *J*, and species, *S*, in a plot of size *A* ($\bar{N} = J/AS$). Damuth's data refer to the number of individuals present per unit of suitable habitat for a particular species. Plots of fixed size *A* may include a mixture of suitable and unsuitable habitats for different species that constitute the communities, resulting in lower estimates for $\bar{N}$.
11. B. J. Enquist, K. J. Niklas, *Nature* **410**, 655 (2001).
12. S. P. Hubbell, *A Unified Neutral Theory of Biodiversity and Biogeography* (Princeton Univ. Press, Princeton, NJ, 2001).
13. J. H. Brown, M. V. Lomolino, *Biogeography* (Sinaur, Sunderland, MA, 1998).
14. M. E. Ritchie, H. Olff, *Nature* **400**, 557 (1999).
15. M. L. Rosenzweig, *Species Diversity in Space and Time* (Cambridge Univ. Press, Cambridge, UK, 1995).
16. R. K. Colwell, D. C. Lees, *Trends Ecol. Evol.* **15**, 70 (2000).
17. D. H. Wright, *Oikos* **41**, 496 (1983).
18. J. F. Gillooly, E. L. Charnov, G. B. West, V. M. Savage, J. H. Brown, *Nature* **417**, 70 (2002).
19. A. H. Gentry, *Ann. Mo. Bot. Gard.* **75**, 1 (1988).
20. B. J. Enquist, K. J. Niklas, *Science* **295**, 1517 (2002).
21. T. Isobe, E. D. Feigelson, M. G. Akritas, G. J. Babu, *Astrophys. J.* **364**, 104 (1990).
22. Mass-corrected population densities for tree species were calculated with the use of a database compiled by Gentry, which includes counts of all individuals ≥2.5 cm in diameter collected from over 200 0.1-ha plots around the world (*19*). Extensive intraspecific variation in plant size required that we use a different approach to calculate mass-corrected population densities for the trees than for the other taxa. We estimated the dry mass (in grams) of each individual, M_j, from its diameter, D_j (in centimeters), using the formula $M_j = 156D_j^{2.53}$ (*11*, *20*). We then computed the average mass-corrected population density as $\overline{NM^{3/4}} = (AS)^{-1} \sum_j M_j^{3/4}$, *where S* is the number of species in the plot of size *A*.
23. D. R. Legates, C. J. Wilmott, *Theor. Appl. Climatol.* **41**, 11 (1990).
24. In Figs. 1 and 2, variation in the dependent variable (abundances of individual species) greatly exceeds errors in the independent variable (temperature) because abundance is known to vary by orders of magnitude among species in a community (*12*). This justifies the use of ordinary least-squares regression (*21*). In Figs. 3 and 4, we used reduced–major-axis regression because errors in the dependent variables (richness) and independent variable (temperature) are likely to be of comparable magnitude.
25. D. Lieberman, M. Lieberman, R. Peralta, G. S. Hartshorn, *J. Ecol.* **84**, 137 (1996).
26. W. E. Duellman, *Ann. Mo. Bot. Gard.* **75**, 79 (1988).
27. K. Rohde, M. Heap, *Int. J. Parasitol.* **28**, 461 (1998).

28. We thank D. J. Currie, T. Oberdorff, and J. T. Kerr for providing data, and D. J. Currie, E. H. Decker, W. Jetz, A. J. Kerkhoff, B. T. Milne, H. Olff, and three anonymous reviewers for comments. We gratefully acknowledge the support of NSF grant DEB-0083422. A.P.A. further acknowledges the support of NSF grant DEB-9910123, and J.H.B. and J.F.G. acknowledge the support of a Packard Interdisciplinary Science Grant.

29 March 2002; accepted 19 July 2002

Geographic Range Size and Determinants of Avian Species Richness

Walter Jetz[1,2]* and Carsten Rahbek[3]

Geographic patterns in species richness are mainly based on wide-ranging species because their larger number of distribution records has a disproportionate contribution to the species richness counts. Here we demonstrate how this effect strongly influences our understanding of what determines species richness. Using both conventional and spatial regression models, we show that for sub-Saharan African birds, the apparent role of productivity diminishes with decreasing range size, whereas the significance of topographic heterogeneity increases. The relative importance of geometric constraints from the continental edge is moderate. Our findings highlight the failure of traditional species richness models to account for narrow-ranging species that frequently are also threatened.

Most analyses of determinants of geographic patterns in species richness have traditionally looked only at overall species richness patterns, but this does not give a representative picture for most taxa. Wide-ranging species contribute many more distribution records to a species richness pattern than do narrow-ranging species. Thus, although most species tend to have range sizes well below average (*1*–*3*), insights from conventional biogeographical analyses of overall species richness are in fact largely based on wide-ranging species. This may produce a profound bias in the presumed determinants of species richness in space that any general model should address.

Determinants of overall species richness singled out so far include measures of productivity (*4*, *5*), habitat heterogeneity (*6*, *7*), area (*8*, *9*), regional and evolutionary history (*10*), synergism between climate and evolutionary history (*11*), and effects from geometric constraints imposed by distribution boundaries such as the continental edge (*12*–*14*). Here we address the potential effect of range size on the pattern of species richness and its presumed determinants (*15*), using a 1°-resolution database summarizing the distribution of the 1599 breeding bird species endemic to sub-Saharan Africa (Fig. 1B) (*15*).

We first examine potential factors one by one, using traditional general linear model (GLM) and spatial linear model (SLM) regression analyses of overall species richness (see table S1 for all single-predictor results). We focus on the latter approach, which avoids inflation of type I errors and invalid parameter estimates due to spatial autocorrelation (*15*–*17*). Our results broadly confirm the important role of net primary productivity (NPP, including a quadratic term, NPP^2) and habitat heterogeneity (HabHet) on species richness asserted in previous studies (*4*–*7*). Both emerge as main predictors of overall species richness (single-predictor SLM: t (HabHet) = 22.03; two-predictor SLM (NPP + NPP^2): t (NPP) = 25.08, t (NPP^2) = –15.62; all $P < 0.001$). These three variables together explain around 66% of the variance (SLM: r^2 of fitted values against observed values, log likelihood = –12,440). Annual precipitation (Rain) also has high predictive value (single-predictor SLM: $t = 26.14$), but because it is strongly collinear with NPP [$r_S = 0.91$, $n = 1738$; two-predictor SLM (NPP + Rain): t (Rain) = 8.69, t (NPP) = 13.66], we did not examine it further.

Other core environmental predictors include topographic heterogeneity [TopHet, measured as altitudinal range; single-predictor SLM: t = 13.77 (table S1)] and mean maximum daily temperature (MaxTemp; single-predictor SLM: $t = -17.74$). In contrast to the suggested direct positive link between temperature as a measure of energy and species richness (*18*, *19*) and some of the empirical findings from South America (*11*), the relationship with maximum temperature is strongly negative: High-temperature quadrats support fewer species than do quadrats with more moderate temperatures. This may suggest an envelope effect of temperature on homeotherms, with both cold and hot temperatures aversely affecting species richness in addition to and conjunction with other factors.

Distribution constraints imposed by continental boundaries, together with the tendency of ranges to be continuous at larger scales of analysis, can demonstrably influence the geography of species richness, with higher levels of species richness expected in the middle of a bounded domain (*12*–*14*, *20*). We found that geometric constraints modeled in two dimen-

[1]Department of Zoology, University of Oxford, Oxford OX1 3PS, UK. [2]Department of Biology, University of New Mexico, Albuquerque, NM 87131, USA. [3]Zoological Museum, University of Copenhagen, Universitetsparken 15, DK-2100 Copenhagen O, Denmark.

*To whom correspondence should be addressed. E-mail: walter.jetz@zoo.ox.ac.uk